Experimental evaluation of the pitch angle righting capabilities of a high speed terrestrial vehicle in ballistic phase

Marc Davis[1,2,a], Philippe Vaslin[1,b], Jean-Christophe Fauroux[2,c], Christophe Gouinaud[1,d], Liang Ju[2,e]

[1]Clermont University, Blaise Pascal University (UBP), UMR CNRS 6158, Computer Science Research Group (LIMOS), Campus des Cézeaux, F-63177 Aubière Cedex, France

[2]Clermont University, French Institute for Advanced Mechanics (IFMA), EA3867, FR TIMS / CNRS 2856, Mechanical Engineering Research Group (LaMI), BP 10448, F-63000, France

[a]marc.davis@isima.fr, [b]philippe.vaslin@isima.fr, [c]jean-christophe.fauroux@ifma.fr, [d]christophe.gouinaud@isima.fr, [e]liang.ju@ifma.fr

Keywords: High speed ballistic robot, pitch angle, angular momentum, moment of inertia

Abstract. We present a study of the feasibility of controlling the pitch angle of a high velocity ground vehicle in ballistic phase by accelerating or decelerating its wheels. The vehicle performed several jumps, and various wheel acceleration commands were sent to it while it was airborne. Images were recorded using a high-speed video camera, and the trajectories of markers placed on the vehicle were analyzed in order to measure the relationship between the changes in angular velocities of the chassis and the wheels. It appeared that it was possible to achieve pitch righting through the modification of the angular velocities of the wheels with adequate performance, thus opening the road towards automated control of pitch, then later yaw and roll angles.

Introduction

High speed terrestrial vehicles can be used in a variety of situations such as mapping and reconnaissance in unknown or hazardous environments, surveillance of vast installations, search and rescue operations, agricultural monitoring, and delivery of critical supplies in humanitarian missions. Even though maneuverability on unstructured terrains at high velocities can be maintained through the use of optimized suspension systems [1], terrain discontinuities and impacts with obstacles can cause ballistic phases which require aerial self-righting if the vehicle is to land with its suspensions facing the ground. In some applications [2], [3], ballistic phases might be voluntary, but still call for attitude correction in order to provide safe landing conditions, and for sending readable real-time images to a remote operator using an on-board camera for first person view control.

The means for enabling aerial self-righting can be derived from techniques evolved in living beings [4], and lizard-inspired solutions [5] have been explored, for example by using a robotic tail to provide pitch righting similarly to techniques used by other reptiles [6]. Traditional self-righting means used in aerospace mainly include the use of thrusters, spin stabilization techniques, reaction wheels, or control moment gyroscopes [7].

Previously, the authors studied this pitch correction maneuver in the case of motocross jumps. A kinematic analysis of video footage taken for this purpose was used to identify the key parameters of this phenomenon. A mechanical model describing the exchange of partial angular momenta between the wheels and chassis was constructed, and numerical analysis in a custom-written 2D Java simulator was conducted so as to study the influence on aerial pitching of back wheel acceleration as well as front and/or back wheel braking [8].

This study focuses on evaluating the controllability of the pitch angle of an airborne vehicle in ballistic phase. After having described the experimental setup and presented the results, the latter will be discussed before concluding this study.

Materials and Methods

The vehicle used for this study is a Traxxas E-Maxx Brushless Model 3908 (Fig. 1a), a 520mm long, 5.2 kg radio-controlled truck capable of reaching velocities of approximately 30 m/s. The vehicle features a four wheel drive powered by a brushless electric motor, and provides a suspension system adapted for recovering from jumps and falls. All four wheels are powered and braked by the motor, which makes this vehicle a good candidate for wheel-based pitch righting, since about 20% of the truck's mass is located in the wheels, and the studied maneuver relies on the exchange of partial angular momenta between the vehicle and its wheels. The front and rear drivetrains are not coupled together by a differential and rotate at the same velocities.

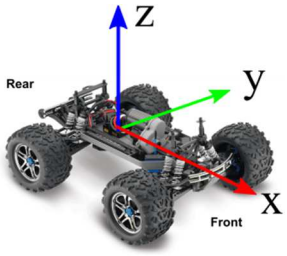

Fig. 1a: The E-Maxx Brushless, with its local reference frame.

Fig. 1b: The ramp at the end of the track, with cones every two meters for calibration, and the vehicle performing a jump.

The experiment consisted in having the vehicle perform three sorts of jumps, with different actions on the throttle, thus on the changes of angular velocity of all four wheels. During "normal" jumps, no commands were sent to the throttle in mid-air; during "accelerated" jumps, the throttle trigger was manually pressed during the aerial phases; during "braked" jumps, the throttle was used to brake the wheels when the vehicle was airborne.

A jumping ramp was installed at the end of a concrete track on a javelin throw field, providing the vehicle with a smooth surface for accelerating towards the said ramp. After jumping, the vehicle would then land on smooth grass (Fig. 1b). Cones were placed at regular intervals in the plane of motion, used for calibrating the horizontal axis in the images to be filmed; the vertical axis was calibrated with a tall object of know dimensions.

The vehicle remote controller was modified so as to enable repeatable input during the acceleration phase on the runway: the throttle trigger was attached to a linkage controlled by a motor, which itself was driven by a Lego Mindstorms NXT control brick (Fig. 2a). Pressing a single on/off button connected to the control brick ensured better angular position repeatability of the throttle than driving the system by hand.

Images were captured with a resolution of 1280x1024 pixels at 500 frames per second using an S-MOTION high speed camera from AOS Technologies [9]. A Pentax K-7 camera was used for filming the ramp itself at 30 frames per second, providing means for measuring the vehicle's velocity upon leaving the ramp (Fig. 2b), and a Pentax K-5 camera was used for filming isometric images.

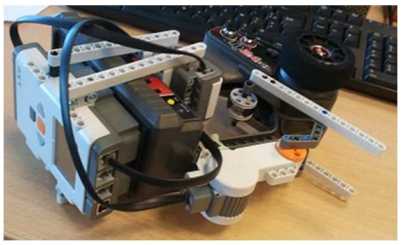

Fig. 2a: The automated vehicle remote control.

Fig. 2b: Measuring take-off velocity with measuring tape on the ramp.

The first set of images captured by the high speed camera was used for spatial calibration of the scene by capturing objects of known dimensions. The scene coordinate system was defined with the **x** axis oriented in the vehicle general horizontal direction of travel (towards the left in Fig. 4), and

the **z** axis towards the sky. All angles measured around the pitching axis (the **y** axis) are thus defined as being increasing in the image counter-clockwise direction.

The image sequences captured with the high speed camera were imported in Vannier-Photolec's MotionTrack video analysis software for tracking the key points on the vehicle. The vehicle attitude was manually tracked as the segment joining the center of both left wheels, and the angular positions of the wheels were automatically tracked by a contrast following algorithm.

The angular positions of the wheels and chassis for the "normal" and "accelerated" jumps were interpolated using sixth degree polynomials, so as to provide angular velocity data in the form of fifth degree functions after differentiation. The angular positions for the "braked" jump had to be interpolated through piecewise functions of degrees one and two.

The moments of inertia of the vehicle and of its wheels were measured using the pendulum method: the objects were suspended by an axis parallel to the pitch axis, and set to oscillate freely by small angle values. Since the period of the oscillations is related to the distance between the pendulum axis and the center of mass, and to the moment of inertia, the latter could be computed once the oscillation period was known [10]. Images were captured at 30 frames per second using a Panasonic DMC-LX2 digital camera, and the markers visible in Fig. 3a and 3b were tracked in the video analysis software mentioned previously.

Fig. 3a: Measurement of the moment of inertia of the vehicle around its **y** axis.

Fig. 3b: Measurement of the moment of inertia of a wheel (150 mm in diameter) around its **y** axis.

The measured moments of inertia were used to compute the total angular momentum of the vehicle in ballistic phase so as to verify the principle of conservation of angular momentum of an isolated system. Eq. 1 gives the expression of the vehicle's total moment of inertia [8]:

$$\overrightarrow{\sigma^*} = J_{G\Sigma y}\overrightarrow{\omega_\Sigma} + \sum_{k=0}^{4} J_{G\mathrm{W}_k y}\overrightarrow{\omega_k}. \quad (1)$$

In Eq. 1, $\overrightarrow{\sigma^*}$ is the total angular momentum of the system around its center of mass, $J_{G\Sigma y}$ is the moment of inertia of the complete vehicle around the pitching axis and $\overrightarrow{\omega_\Sigma}$ is the angular velocity of the vehicle. $J_{G\mathrm{W}_k y}$ is the moment of inertia of wheel number *k* around its axis of rotation, and $\overrightarrow{\omega_\mathrm{k}}$ is the angular velocity relative to the local reference frame of wheel number *k*.

Results

In the "normal" jump (Fig. 4a), it appears that the vehicle's attitude varies very little between positions 1 and 3, and that the vehicle pitches very slightly in the negative direction (clockwise) before landing safely in pos. 7. The vehicle throttle might have been involuntarily actuated during the whole jump, resulting in the observed motion. This jump is thus a very slightly accelerated jump.

In the "accelerated" jump (Fig. 4b), the vehicle pitch angle varies very little until pos. 2 (throttle was possibly still being applied), then abruptly changes as the throttle is pressed and the wheels accelerate around pos. 3. It is to be noted that the tires seem to have bulged due to the centrifugal effect in pos. 7 to a diameter larger than in pos. 1.

In the "braked" jump (Fig. 4c), the vehicle seems to be in pure translation at pos. 2, 3 and 4, then the brakes are applied shortly after pos. 4, and the vehicle pitches forward in the positive direction.

a)

b)

c)

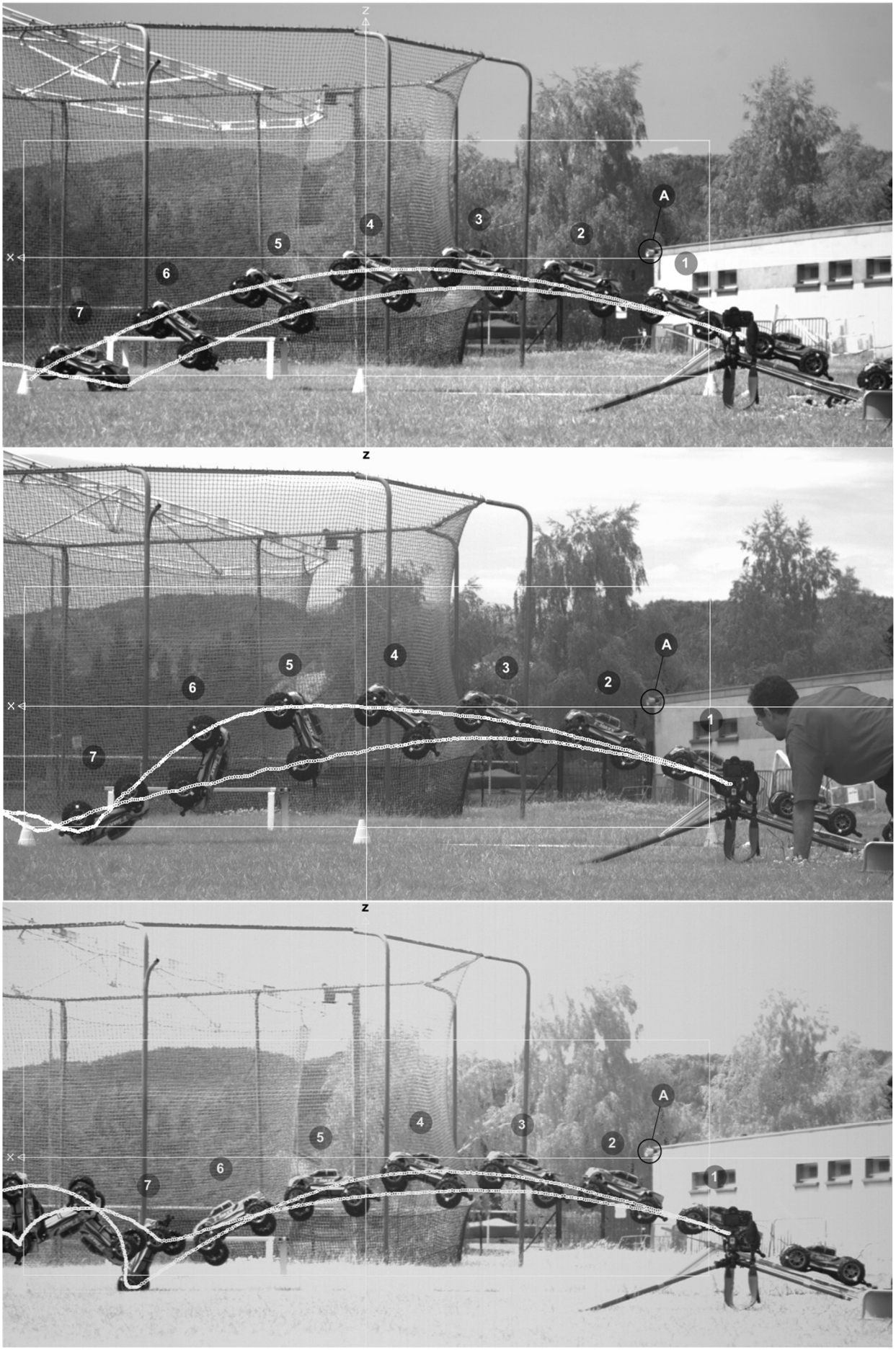

Fig. 4: A “normal” jump (a), an “accelerated” jump (b) and a “braked” jump (c).

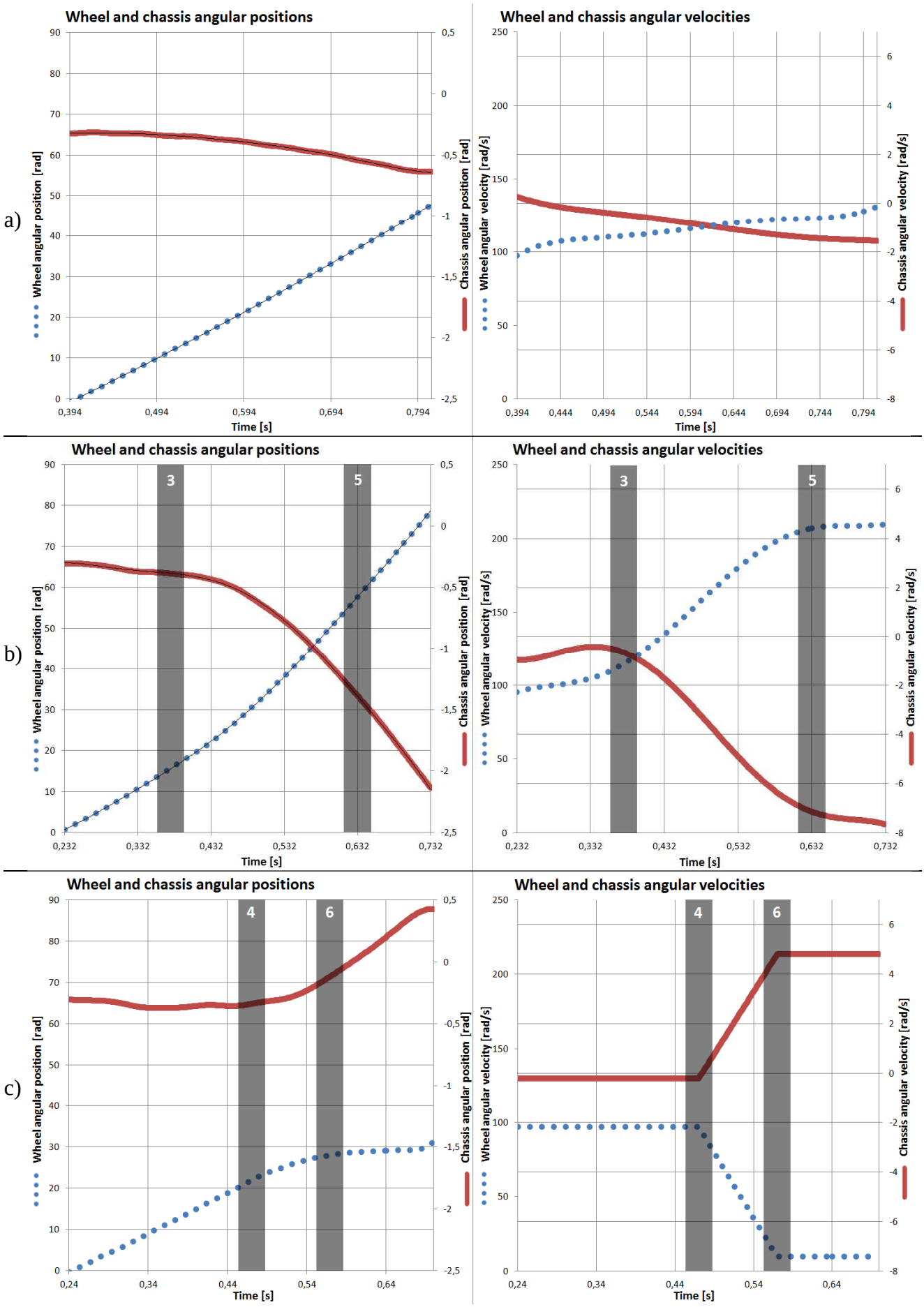

Fig. 5: Angular positions (left column) and angular velocities (right column) of the wheels and chassis during a “normal” jump (a), an “accelerated” jump (b) and a “braked” jump (c).

Figure 5 displays the raw and interpolated angular positions for each jump, as well as the angular velocities obtained through differentiation of the interpolated positions. The "normal" jump (Fig. 5a) exhibits a slight angular acceleration throughout the ballistic phase. The remote control throttle was set close to zero, but it appears that a slight acceleration command was still being sent. However, the acceleration seems constant, and while the wheels undergo a positive acceleration, the vehicle nose pitches up as expected.

During the "accelerated" jump (Fig. 5b), it appears that an acceleration command was sent around pos. 3, and stopped around pos. 5. While the throttle was set to its maximum value gradually (not in an abrupt manner), the vehicle's angular velocity decreased by 5.2 rad/s in about 0.2s, yielding an angular acceleration of -22.2 rad/s². At that rate of acceleration, the vehicle could be capable of modifying its pitch angle by half a turn in 0.53s.

During the "braked" jump (Fig. 5c), the brakes were applied gradually from around pos. 4 to pos. 6. The vehicle angular velocity increased by 4.8 rad/s in 0.01s, yielding an acceleration of 50.2 rad/s². While this angular acceleration is only available until the wheels come to a stop, it would have been possible to lengthen this forward pitching maneuver by accelerating the wheels in reverse gear after the braking was completed.

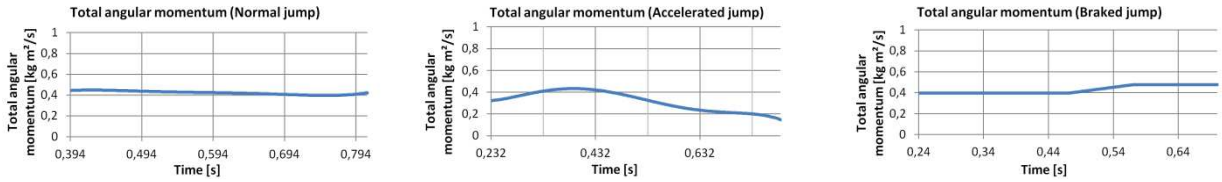

a) b) c)

Fig. 6: Total angular momentum of the "normal" (a), "accelerated" (b) and "braked" (c) jumps.

Overall, it appears that using the vehicle wheels for pitch righting maneuvers is completely feasible, and that the potential for executing these maneuvers is present for even the most extreme cases and initial conditions.

For the sake of verifying the data against the mechanical model, the moments of inertia of the vehicle and its wheels were measured and used in Eq. 1 along with the relevant angular velocities for each jump in order to compute the system total angular momentum. While the calculated values were found to be close to constant (Fig. 6) during the ballistic phases, variations were still observed, which violates the law of conservation of angular momentum. The maximal error in total angular momentum relative to its average value was of 6.15% for the normal jump, 36.9% for the accelerated jump and 11.8% for the braked jump. These variations could be caused by a number of factors, which will be discussed in the next section.

Discussion

The results of this study are subject to measurement errors emanating from multiple sources, and which can be divided into two categories [11]: random errors and systematic errors. Random errors fluctuate in an unpredictable manner, and can be diminished by repeating the same measurement in the exact same conditions multiple times. Systematic errors are those introduced by the methods of measurement, the operators, the hardware used, the environment and the objects being measured. Many factors were identified as being possible sources of error, and they were found to be almost exclusively of systematic nature. A quantification of the amount of random error will be presented in the next section, followed by the discussion of several sources of systematic error.

Random Errors. They have a multitude of possible causes, which can include camera sensor noise, transient changes in illumination of the objects, camera vibrations, dust particles passing in front of the lens, errors in the software contrast tracking algorithm and various round-off errors.

In order to quantify these random errors, a stationary marker in the scenes was filmed (Fig. 4, pos. “A”). This marker was chosen because of the similarity in contrast and size to the markers to be followed on the vehicle. In future studies, markers identical to those to be tracked on the truck

will be placed on stationary surfaces for random error measurement and for scene calibration. The marker was automatically tracked by the video analysis software during a whole jumping sequence.

The raw **x** (horizontal) and **y** (vertical) pixel coordinates of the marker were extracted (Fig. 7), and it appears that the **x** coordinates fluctuate in a range of 0.6 pixels (0.05% of the camera field in the **x** direction), while the **y** coordinates vary in a range of 1.4 pixels (0.14% of the camera field in the **y** direction). It is interesting to note that the random errors are not equal in their vertical and horizontal distributions, which could be caused by the fact that since the tracked object was wider than tall, pixel value errors had less impact on the computed center of the object in the **x** direction than in the y direction. These random errors were deemed to be negligible relatively to the sources of systematic uncertainty which will now be presented.

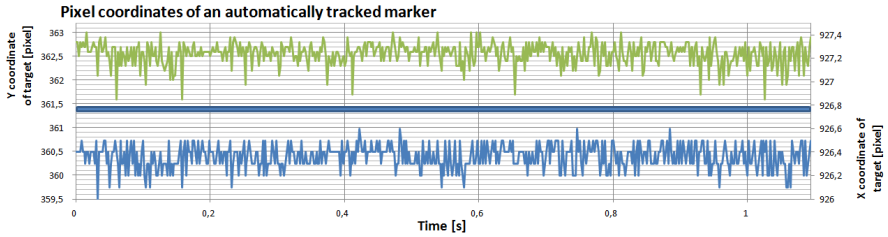

Fig. 7: Raw **x** (bottom curve, left scale) and **y** (top curve, right scale) pixel coordinates of a stationary marker.

Tracking of Markers on the Wheels. Markers on the wheels were materialized by square pieces of white tape placed on the tires, and these markers were automatically followed by the video analysis software. Initial measurements of the wheel and chassis angular velocities proved to be undulating around the expected values, with a frequency equal to that of the wheels rotation.

It was decided to measure the evolution of a supposed constant, the radius of the wheels, defined as the distance between the markers in the centers of the wheels and the markers at their peripheries. It was found that instead of being constant, this distance varied significantly. While the average value of the radius was measured at 55mm, the actual values oscillated in an 18mm range around that average (Fig. 8a).

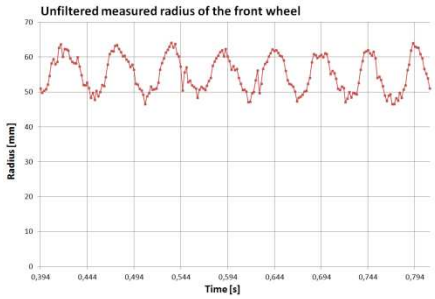

Fig. 8a: Measured wheel radius variation.

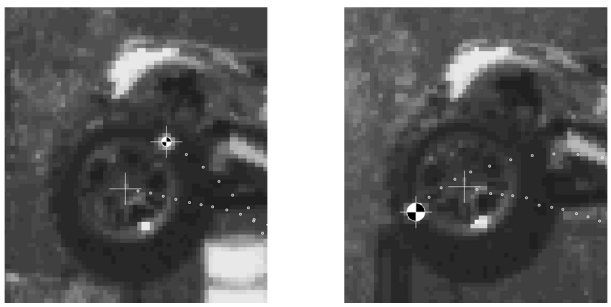

Fig. 8b: Variation in wheel marker size.

This change in measured radius is cyclical and depends essentially on the wheel's angular position; it could have several causes. Firstly, the background of the markers being the tires themselves, the contrast between the markers and the rubber varied with the angular position relative to incident sunlight. Secondly, the markers being square, their shape varied continuously in terms of discrete pixel representation, thus leading the automatic contrast following algorithm to introduce uncertainties on the marker sizes and geometric centers. Thirdly, the markers having been placed on curved shapes non perpendicular to the camera axis, the projected and pixel-discrete sizes of the markers in the camera focal plane varied with each rotation as well. All these variations led the video analysis software to consider the markers to be varying in size (Fig. 8b), and introduced large errors which propagated undulating errors in every subsequent calculation. In future work it will be necessary to use markers of appropriate shape, size, contrast, placement, background and orientation relative to the camera and to the light source in order to reduce this behavior. This

source of error called for the use of polynomial interpolation of the angular positions of the wheels and chassis.

Polynomial Interpolation. Because the main source of error in the measurements was by nature of the same frequency than that of one of the phenomena to be measured, it was impossible to isolate and filter out that frequency without severely distorting the data from its actual meaning. It was decided to use polynomial interpolation as a temporary solution for succeeding in observing the relationship between the chassis and wheel angular velocities. The angular positions were interpolated, and the obtained polynomials were differentiated in order to obtain angular velocities. This solution enabled for the extraction of adequate tendencies concerning the phenomenon, but proved to have its limits. High polynomial degrees introduced parasite undulations on the interpolated data, and low degrees caused severe loss of fidelity, even more so once the polynomials were differentiated. In the case of the braked jump, curve fitting was simply not acceptable, and the obtained angular velocities lost all meaning, thus leading to the use of first and second degree curves for tendency extraction. In future work it is expected to obtain data with much less of the cyclical noise measured in this work, enabling the use for more traditional and refined filtering methods.

Marker Placement. It was chosen to measure the vehicle attitude using the wheel centers, since the objective is to correct the vehicle attitude so that a plane tangent to its four wheels becomes parallel to the ground before landing. However, it appears that the vehicle suspensions are excited during the jumps, as visible on the angular position curves of the “accelerated” jump (Fig. 4b, pos. 5 and 6). In order to be able to measure the actual angular momentum of the vehicle, it is necessary to measure the wheel position relative to the chassis, thus introducing the need for markers on the chassis itself.

Moments of Inertia. The experimental conditions for measuring an object’s moment of inertia while minimizing measurement errors are known [12]: the distance between the center of mass of the object and the rotation axis is optimal when it is slightly less than the radius of gyration. However these conditions are not always easily applicable: the localization of a usable pivot axis is not always trivial, and the measurement of the distance of that axis to the vehicle center of mass is a potential source for error. Moreover, it was observed that the wheels change in shape and diameter as a function of their angular velocity (Fig. 9). This necessarily introduces changes in their moments of inertia, which must be either modeled and taken into account, or mechanically forbidden.

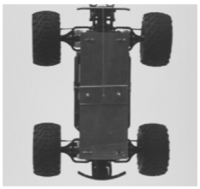

Fig. 9a: The wheels at rest

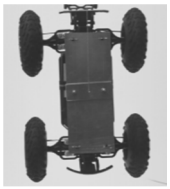

Fig. 9b: The wheels bulging at high velocity

Fig. 9c: Left tires spinning and bulging while right tires adhere

Scene Lighting. The Sun was the primary light source during the tests. While before each jump the high speed camera exposure settings were adjusted, changes in illumination conditions took place between the end of the adjustment and the actual filming of the sequences. While the human eye could hardly notice the subtle changes in lighting due to the changing thickness of the cloud cover, the camera sensor eventually produced over-exposed images. As an effect, contrast following proved difficult in some captured sequences. Subsequent manipulations should be either artificially-lit, or camera exposure should be set when the sky is clear and it is certain that no clouds could block the Sun at the time of capture.

Jump Initial Conditions. While the vehicle throttle was automatically actuated as it approached the ramp, steering was done manually and uncertainties on the jump initial conditions could have been introduced. As a result, the parabolic motion of the center of mass of the vehicle could have taken place in a different plane than that used for calibrating the scene, thus inducing errors in

distance measurements. Moreover, slight steering commands may have been sent to the vehicle while it was on the ramp, causing it to have initial yawing and rolling motions during the jumps. Fig. 10 displays various positions of a vehicle initially meant to perform a “normal” jump. In this case, one of the wheels was not actually on the ramp during takeoff, introducing a great amount of yawing on the vehicle during the ballistic phase.

Fig. 10: Strong yawing initial conditions

In the case of the “braked” jump (Fig. 4c), the vehicle appears to exhibit a slight amount of rolling motion in the positive direction, possibly introduced by initial conditions set by the approach parameters. In order to eliminate this problem it could be necessary to automate to some extent the vehicle steering, for example by following a painted line, or by taking readings from a compass or magnetometer. Another solution would be to use a second camera for stereo vision, enabling the reconstruction of actual trajectories in 3D, as well as the tracking of not only pitching, but also rolling and/or yawing motions.

Control Law during Ballistic Phases. The throttle and brakes were manually actuated during the jumps, leaving no indication of what the actual commands were, and of their timing. While the commands can be inferred from the measurements of the wheel velocities, they are still not explicitly known. Moreover, it would have been interesting to have the commands be automatically applied directly after takeoff, thus lengthening the duration of their application.

Conclusion and Future Work

In this work, we demonstrated that it was feasible to modify the pitch angle of a four-wheeled vehicle around its center of mass during an expected aerial phase using wheel acceleration or braking. The acceleration and braking were only applied during a short time frame with respect to the total ballistic phase but their effect was quite pronounced with a standard brushless engine. The forward pitching motion during the braked jump was only achieved through engine braking and could be intensified by reverse acceleration of the wheels.

A high speed camera was successfully applied for the measurement of the vehicle pitch angle and wheel angular position during flight. A certain amount of noise was observed on the angular data, requiring the careful choice of filtering methods for eliminating it without deforming the actual trajectories. For subsequent tests, specular reflections have to be suppressed and markers of appropriate size and contrast must be placed on a flat surface of the rim, thus avoiding problems from tire deformation, cyclic changes in illumination conditions and partial cyclic occlusion of the targets. Vehicle attitude should also be measured using markers on the chassis rather than at the center of each wheel. Moreover, tire bulging due to the centrifugal force must either be modeled or be inhibited. These improvements will hopefully allow us to observe the expected constant nature of the total angular momentum.

Future work will focus on implementing the automatic control of the pitch motion, using proprioceptive sensors and a very fast embedded control loop. As the jumps can last well under a second (typically 0,2 s), the control loop is expected to be able to run at least at 1 kHz. A second task will be to correct also the yaw and roll angles with the same constraints, the long term goal being to enable the vehicle to achieve actual 3D self-righting, which would require the use of high-speed stereo vision for the experimental aspects.

The previous ANR FAST project led to the design and control of the suspensions of a vehicle meant to maintain its stability at high speed on irregular terrains. The current RobCat project extends these capabilities also to ballistic phases. Combining both will allow to design and control a

fully autonomous agile robot capable to move and jump at high speeds over unstructured terrains for surveillance, mapping, agricultural, search and rescue, and humanitarian tasks.

Acknowledgements
This work was financed by Région Auvergne through the "Innov@Pôle" project. It was supported by the "Fédération de Recherche Technologies de l'Information de la Mobilité et de la Sûreté" (FR TIMS, CNRS 2856), and its "Véhicules et Infrastructures Intelligents" (V2I) project (for the "RobCat" project). This federation is supported by the French Ministry for Higher Education and Research, the Agence Nationale de la Recherche (for the ANR FAST project), Région Auvergne, and the "Europe en Auvergne" FEDER (Fonds Européen de DÉveloppement Régional) program.

The authors wish to thank Issam Rajib and Samir Belazouz, who were of great help in conducting the experiments. Lastly, we wish to thank Christine Dulac-Rougerie, Deputy Mayor of Clermont-Ferrand in charge of Sports, Outdoor Leisure and Vacation Centers, David Rocton, director of the Stadium Jean Pellez in Aubière, as well as the whole staff of the Stadium for having authorized and enabled the use of their sports installations for our tests.

References

[1] J.C. Fauroux, J. Dakhlallah, B.C. Bouzgarrou, A New Concept of FAST Mobile Rover with Improved Stability on Rough Terrain, in Proc. of HUDEM'2010, 8th International Advanced Robotics Programme (IARP) Workshop on Robotics and Mechanical assistance in Humanitarian De-mining and Similar risky interventions, 10-12 May, 2010, Nat. Eng. School of Sousse, Tunisia. Paper #26, 16 p. Downloadable on http://jc.fauroux.free.fr.

[2] D. Hurst, Sandia hopping robots to bolster troop capabilities, Sandia Labs News Releases, 11-Sep-2009. [Online]. Available: http://goo.gl/YuzlO.

[3] M. Hoffman, Jumping robot to get tested in Afghanistan, ArmyTimes, 07-Nov-2011. [Online]. Available: http://goo.gl/gvhCt.

[4] M. Davis, C. Gouinaud, J. C. Fauroux, and P. Vaslin, A Review of Self-Righting Techniques for Terrestrial Animals, in International workshop on bio-inspired robots, Ecole des Mines and IRCCYN LAB, Nantes, 2011.

[5] E. Chang-Siu, T. Libby, M. Tomizuka, and others, A lizard-inspired active tail enables rapid maneuvers and dynamic stabilization in a terrestrial robot, in Intelligent Robots and Systems (IROS), 2011 IEEE/RSJ International Conference, 2011, pp. 1887–1894.

[6] A. Jusufi, D. I. Goldman, S. Revzen, and R. J. Full, Active tails enhance arboreal acrobatics in geckos, Proceedings of the National Academy of Sciences, vol. 105, no. 11, pp. 4215 -4219, Mar. 2008.

[7] C. Kaplan, LEO satellites: attitude determination and control components; some linear attitude control techniques, Master of Science in Electrical and Electronics Engineering Thesis, Middle East Technical University, 2006.

[8] P. Vaslin, V. Pouzols, C. Gouinaud, J.-C. Fauroux, S. Deleplanque, and M. Davis, Contrôle du tangage d'un véhicule en phase balistique, in 20ème Congrès Français de Mécanique, Besançon, 2011.

[9] AOS Technologies AG, S-MOTION High Speed Camera Technical Specifications. [Online]. Available: http://goo.gl/P3qJX.

[10] V. Pouzols, Modélisation des facteurs influençant la trajectoire aérienne du système {pilote + moto} lors d'un saut en moto-cross. Validation expérimentale du modèle, Master of Science in Mechanics, Université Blaise Pascal, Clermont-Ferrand, 2006.

[11] Mouvement Français pour la Qualité, Guide pour la détermination des incertitudes de mesure, MFQ Franche Compté, Besançon, 1995.

[12] J. J. Dowling, J. L. Durkin, and D. M. Andrews, The uncertainty of the pendulum method for the determination of the moment of inertia, Medical engineering & physics, vol. 28, no. 8, pp. 837–841, 2006.